Erosional response to land abandonment in rural areas of Western Europe during the Anthropocene: A case study in the Massif-Central, France

Anthony Foucher, O. Evrard, Clément Chabert, Olivier Cerdan, Irène Lefèvre, Rosalie Vandromme, Sebastien Salvador-Blanes

Erosional response to land abandonment in rural areas of Western Europe during the Anthropocene: a case study in the Massif-Central, France

Anthony Foucher [1,2], Olivier Evrard [1], Clément Chabert [1,3], Olivier Cerdan [3], Irène Lefèvre [1], Rosalie Vandromme [3], Sébastien Salvador-Blanes [2]

[1] Laboratoire des Sciences du Climat et de l'Environnement, (LSCE), UMR 1572 (CEA/CNRS/UVSQ) – Bâtiment 714, Ormes des Merisiers, F-91191, Gif-sur-Yvette Cedex, France

[2] Laboratoire GéoHydrosystèmes Continentaux (GéHCO), E.A 6293, Université F. Rabelais de Tours, Faculté des Sciences et Techniques, Parc de Grandmont, 37200 Tours, France

[3] Département Risques et Prévention, Bureau de Recherches Géologiques et Minières (BRGM), 3 avenue Claude Guillemin, 45060 Orléans, France

Abstract

Abandonment of agricultural land is widespread in many developed countries. These surfaces are projected to increase significantly worldwide during the 21th century. Identifying potential relationships between land abandonment and soil erosion dynamics over the long term (100 years) is therefore essential for predicting the environmental consequences of this extensive land use change. Accordingly, sediment cores were collected in two highland catchments of central France in order to reconstruct the change of sediment delivery during the last century. The results showed a substantial decline (71-78%) of rural population in both sites since 1900. This decrease occurred simultaneously with a sharp decline (85–95%) of the surface of arable land: previously cultivated areas were mainly converted into forests as the result of natural and anthropogenic processes. Consequently, sediment deliveries significantly decreased (75–99%) in both catchments. These trends were nevertheless interrupted by the implementation of afforestation works between 1945 and 1970 in one of the catchments. During these works, erosion rates increased three-fold because of extensive soil disturbance, and sediment delivery stabilized only 15 years after the onset of these management operations. Overall, this study demonstrates the long-term effect of land abandonment on soil erosion, which supplements the more widely reported acceleration trend of soil erosion because of agricultural intensification.

Keywords: land use change, afforestation, erosion decrease, highland catchment, depopulation

1. Introduction

Human activities have induced major land use changes during the 20th century worldwide (Foley et al., 2005). Natural landscapes were often converted for practicing intensive agriculture (Antrop, 2005). At many places, the drainage network across the landscape was strongly modified, with the design of streams, ditches, tile drain networks, irrigation systems and the development of landscape planning (Feder and Umali, 1993). These changes in management resulted in the significant increase in the average farm size, mainly in developed countries, and in the expansion of the agricultural areas at the expense of wetlands, forested and drier areas (Klein Goldewijk et al., 2016).

In contrast, economically unproductive areas were increasingly abandoned or reforested as a result of natural or anthropogenic processes. According to the literature, land abandonment mainly occurred in developed countries (Queiroz et al., 2014). During the 20th century, land abandonment was mainly reported from North America, the former Soviet Union and, to a lower extent, from Europe, Japan, Australia and China since the 1960s (Cramer et al., 2008). Land abandonment may result from the combination of various drivers including environmental (e.g. decline of soil fertility and productivity), social (e.g. depopulation in rural areas), economical (e.g. agriculture globalization, adjustment to the open-market) and political factors (Cramer et al., 2007; Lesiv et al., 2018).

The relationship between soil erosion and land use change is well documented in intensive agricultural areas (Boardman and Poesen, 2006; Kosmas et al., 1997), but very few records are available to quantify the link between landscape abandonment and soil erosion during the last century (e.g. Arnaez et al., 2011). However, the investigation of this issue is of paramount importance as the total area of farmland abandoned during the 20th century was estimated to 8-10% of the cultivated areas in the world in 2012 (Campbell et al., 2008), (i.e. 1.5 million km² (Navin Ramankutty and Foley, 1999). Furthermore, the surface area of

77 abandoned lands is projected to further significantly increase during the 21th century
78 (Keenleyside and Tucker, 2010).

79 In this context of projected increase of abandoned land, a better understanding of the
80 links occurring between landscape characteristics, land use change and sediment delivery is
81 required. Among most of the studies that investigated these relationships, their analyses were
82 based on model applications, field observations and they were mainly conducted in specific
83 areas. Among these regions, Eastern Europe and Mediterranean area were the most
84 investigated (e.g. García-Ruiz and Lana-Renault, 2011; Rodrigo-Comino et al., 2018). In
85 particular, studies were conducted on Mediterranean terraces (Koulouri and Giourga, 2007;
86 Lesschen et al., 2008), desertification processes (Hill et al., 2008), carbon sequestration
87 (Novara et al., 2017; Schierhorn et al., 2013) or again on the impact of land abandonment on
88 biodiversity and ecology (Plieninger et al., 2014; Queiroz et al., 2014).

89 The temporal window covered by the available studies is generally relatively short as they
90 were often restricted to the last 40-50 years (Lasanta et al., 2017), mainly because of a lack of
91 past land use information (e.g. aerial imagery).

92 To the best of our knowledge, there have been few attempts – if any – to reconstruct these
93 relationships continuously during the Anthropocene in abandoned highland areas through the
94 analysis of sedimentary sequences. Although the analysis of sediment cores is a powerful
95 technique to reconstruct continuous and high resolution information on sediment inputs and
96 erosion rates in ungauged catchments (Dearing and Jones, 2003), these approaches were
97 almost exclusively conducted in ponds and lakes draining intensive agricultural environments
98 during the last century (Foucher et al., 2017; Heathcote et al., 2013). Many studies were also
99 conducted in high altitude lakes to reconstruct the processes that occurred during the entire
100 Holocene (Bajard et al., 2016; Giguet-Covex et al., 2011), and they therefore investigated
101 very different processes.

In the current research, sedimentary sequences were collected in two contrasted highland catchments of central France (Massif Central). These sites were selected in order to reconstruct the impact of land abandonment induced by depopulation on sediment delivery during the Anthropocene. Overall, the objective of the current project was to better understand the links between rural depopulation, land use change and the evolution of sediment delivery.

2. Sites and methods

2.1 Study sites

Two study sites representative of those contrasted trends of land cover change were selected across the Loire River basin (117,500 km²) - (Fig. 1). Both catchments are located in the low mountain range area of the Massif Central (average elevation: 714m a.s.l; peak: 1885 m a.s.l).

Prugnolas Catchment description

The Prugnolas site (45.868518N, 1.902714E) is a 7.8km² headwater catchment located on the southwestern edge of the Loire river basin (Fig. 1). The distribution of the soil types in the catchment follows that of the two main morphological areas corresponding to the leucogranitic slopes and the talwegs. On the leucogranitic slopes, the mains soils are epileptic Umbrisols developed on leucogranite on the upper slopes, hyperdystric cambic Umbrisols developed on weathered leucogranite on the lower slopes and hyperdystric Cambisols developed on colluvium on the toeslopes. Within the thalwegs, soils are mainly fibric or sapric Histosols and Gleysols (INRA, 2015; IUSS Working Group WRB, 2015). The climate of this region is humid and oceanic: average annual precipitation amounts to around 1550 mm. Elevation ranges between 660 and 830 m a.s.l, with an average slope of 12%. Current

126 land use is mainly dominated by forests (82%), followed by natural grassland and managed
127 grassland (16%).

128 The catchment's river network drains into a pond created in 1645 A.D at the outlet.
129 This 1.8ha north-south oriented water body is a shallow environment (average water depth
130 0.65m) with a maximal water depth of 1.5m close to the dam. To the best of our knowledge,
131 dredging operations were never conducted in this pond during the 20th century, although it
132 was emptied on two occasions, i.e. in 1971 and in 1978.

133 *Malaguet Catchment description*

134 The Malaguet site (45.250578N, 3.713049E) is a small headwater catchment (3.7km²)
135 located along the southern edge of the Loire River basin (Fig.1) Soils are underlain by a mix
136 of hyperdystric Cambisols (IUSS Working Group WRB, 2015). Elevation ranges between
137 1025 and 1127m a.s.l, with a mean slope of 7.5%. Average annual rainfall in this area
138 amounts to 796mm, which is characteristic of a temperate continental climate. Current land
139 use is dominated by forests (71%) and grassland (13%).

140 The 2.7-km long river network drains into a medieval pond (1381AD) of 20.5ha at the
141 catchment outlet. This northwestern-southeastern oriented water body has an average depth of
142 2.8m with a maximal water depth of 4.4m close to the dam, in the southeastern part (Fig. 1).
143 To the best of our knowledge, this pond was never drained during prolonged periods.

144

145 *2.2 Materials and methods*

146 A 77 cm-long sediment core [43MA1703] was collected at 3m depth in the central part
147 of the Malaguet lake and a 70 cm-long sediment core [23PR1701] was retrieved in the deepest
148 part (0.9cm depth) of the Prugnolas pond. Sampling locations were selected in order to be
149 representative of those sedimentary inputs at both sites. Core collection was performed using
150 a floating platform and an Uwitec gravity corer equipped with a 90 mm PVC liner (Fig. 1).

151 Sample locations and bathymetric data were collected using a Garmin *Echomaps* depth
152 sounder.

153 *Laboratory analyses*

154 Relative sediment density was recorded every 0.6mm along the sediment sequences
155 using Computer Tomography (CT-scan) images obtained using those facilities (Siemens
156 Somatom 128 Definition AS scanner) available at the CIRE platform (Surgery and Imaging
157 for Research and Teaching; INRA Val de Loire, France). Relative density values were
158 extracted from the scanner images using the free software ImageJ (Schneider et al., 2012).
159 The relative values of density were calibrated by measuring the absolute dry bulk density
160 ($g.cm^{-3}$) in 25 samples collected randomly along the core.

161 X-Ray Fluorescence (XRF) measurements were obtained with an Avaatech core
162 scanner (EPOC Laboratory, Bordeaux University, France). High density records (every
163 0.5mm) provided relative information on the sediment geochemical content (expressed in
164 counts by second (cps)). The K/Ca ratio characterizing the evolution of the contribution of
165 terrigenous material to the sediment was calculated for both ponds (Croudace and Rothwell,
166 2015).

167 *Sediment core dating*

168 The chronology of sediment accumulation was established for both sites using the
169 measurements of excess Lead-210 ($^{210}Pb_{ex}$) and Caesium-137 (^{137}Cs) in 32 samples
170 (respectively 15 and 17 samples for the Prugnolas and Malaguet sites) of dried sediment
171 (~10g). These gamma spectrometry measurements were obtained with the very low
172 background GeHP detectors available at the Laboratoire des Sciences du Climat et de
173 l'Environnement (Gif-sur-Yvette, France). Radionuclide activities were decay-corrected to
174 the sampling date (Evrard et al., 2016b).

175 Ages were determined using the Constant Rate of Supply model (CRS) (Appleby and
176 Oldfield, 1978). This model assumes variations in the rate of sediment accumulation despite a
177 constant rate of $^{210}Pb_{ex}$ from the atmospheric fallout. The age model based on $^{210}Pb_{ex}$ records
178 was validated through the identification of ^{137}Cs peaks in the sediment sequences, as two main
179 sources supplied this artificial radionuclide in soils and sediment of Western Europe, i.e.
180 thermonuclear weapons testing (with an emission peak in 1963), and the Chernobyl accident
181 in 1986. Dating of the Prugnolas pond sediment core (23-PR-1701) is described in details in
182 Foucher et al. (in prep).

183 *Calculation of mass accumulation rates*

184 Mass accumulation rate (MAR expressed in $g.cm^{-2}.yr^{-1}$) used to quantify the mass of
185 sediment deposited for each time and surface unit was calculated as follows:

186 $MAR\ [g.cm^{-2}.yr^{-1}] = SAR \times DBD$

187 DBD corresponds to the dry bulk density ($g.cm^{-3}$) estimated with the ultra-high resolution
188 calibrated CT-Scan data. SAR, expressed in $cm.yr^{-1}$, corresponds to the sediment
189 accumulation rate estimated with the corrected CRS age model. This equation provides the
190 total flux of material deposited in the reservoir, including both the production of organic
191 material within the lake and the supply of terrigenous material from the catchment.

192

193 *Evolution of land use and population*

194 Past land use was reconstructed based on digitized aerial images and statistical records
195 available from the French agricultural census. For the Malaguet site, eight series of aerial
196 images taken in 1948, 1955, 1967, 1977, 1985, 1995, 2005 and 2013 were available. For the
197 Prugnolas catchment, five series were retrieved (in 1950, 1968, 1972, 1979, 2010). Only 5
198 land use classes, easily identified on the pictures, were documented: water bodies, forests,
199 arable land, grassland and urban settlements. Additional data on the land cover were derived

200 from the agricultural census (e.g. dominant crop types, discrimination between permanent and
201 temporary grassland). These data were available in 1955, 1970, 1979, 1988, 2000 and 2010.
202 Both datasets were combined to obtain a continuous time series during the 1948-2010 period.
203 In addition, the evolution of population in both catchments was reconstructed for the
204 1901-2015 period, based on those French demographic censuses conducted every 6 years.
205 Data were only lacking for those World War periods between 1914-1918 and 1939-1945.
206 *Statistical analyses*
207 The Mann-Kendall non-parametric test (MK-test) was used for detecting monotonic
208 trends in temporal series (Warren and Gilbert, 1988) and it confirmed the occurrence of
209 monotonic upward or downward trends of a given variable throughout time (with a *p*-value
210 level of 0.05). Trends can be positive, negative or non-null.
211 Then, the non-parametric homogeneity test (Buishand test) was used for detecting the
212 occurrence of changes in temporal series (Buishand, 1982). Buishand test with a *p*-value
213 <0.05 indicated a non-homogenous temporal trend between two periods.
214 Finally, the Mann-Whitney (MW-test) non-parametric test was used for detecting statistical
215 differences between two sets of variables. MW-tests with a *p*-value <0.05 indicate a statistical
216 difference between the variables.
217
218 **3. Results**
219 3.1 Evolution of population
220 Analysis of the demographic data showed the occurrence of a constant decrease of
221 population in both catchments. These trends were statistically significant (MK test; *p*-value
222 <0,001) – (Fig. 2). In Prugnolas, the population decreased from 1002 inhabitants in 1901 to
223 218 in 2015, corresponding to a decline of 78%. The Buishand test (*p*-value <0,001) indicates
224 the occurrence of two periods of significant change during this period, respectively in 1918

225 and in 1984. For the Malaguet catchment, similar observations were made. Population
226 declined by 71%, from 1402 inhabitants in 1901 to 399 in 2015. As for the Prugnolas
227 catchment, the Buishand test identified two periods of significant change, in 1916 and in
228 1979.

229 These values illustrate the progressive depopulation of both catchments during the 20th
230 century. This rural depopulation accelerated after WWI and continued until the 1980s. The
231 trends found in these rural areas are in opposition with those observed at the national level,
232 with a significant increase of the total population in France after WWII (Fig. 2).

233

234 3.2 Evolution of land use

235 In the Prugnolas catchment, the proportion of agricultural land (both cropland and
236 grassland) decreased throughout time (MK-test *p*-value <0,001) – (Fig. 3). The surface
237 dedicated to agricultural production (livestock and cereal production) decreased by 76% in 60
238 years. In particular, the cropland surface area which amounted to 7.3% of arable land in 1950,
239 decreased to only 0.4% in 2010 (95%-decrease). During the same period, grassland surface
240 decreased by 74%. Agricultural land was mainly replaced with forest. Forested and
241 abandoned grassland characterized by the regrowth of trees increased by 173% between 1950
242 and 2010 (covering respectively 30% of the catchment surface area in 1950 and 82% in
243 2010). Figure 4 shows the temporal evolution of the spatial pattern of forested surfaces in this
244 catchment during the second half of the 20th century. The Buishand test indicates the
245 stabilization of these land use proportions from 1970 onwards.

246 For the Malaguet catchment, the proportion of agricultural land (cropland and
247 grassland) also decreased throughout time (MK-test *p*-value <0,001). The surface dedicated to
248 agricultural production was divided by 3 between 1948 and 2010 (decreasing from 45 to 15%
249 of the catchment surface) - (Fig. 3). In particular, cropland areas decreased from 85% in 55

250 years (covering respectively 13% of the surface in 1955 against 2% nowadays). Cropland was
251 mainly replaced with permanent/temporal grasslands. The surface of the permanent area
252 under grass increased respectively from 67% to 88% of the agricultural surface during the
253 second half of the 20th century. In parallel to the decline of agricultural land, the proportion of
254 forested areas rose by 67% between 1948 and 2010 (increasing respectively from 43% to 72%
255 of the catchment surface). This increase illustrates the occurrence of reforestation since 1955
256 (*p*-value <0,05) – (Fig. 3).
257 Both catchments showed the progressive encroachment of the landscape with woodland
258 during the second part of the 20th century, mainly through afforestation and/or conversion of
259 cropland into grassland or unmanaged forests.
260
261 3.3 Sediment dating
262 Dating of the Prugnolas sediment sequence was detailed in Foucher et al. (in prep). This
263 archive covers the sedimentation processes that occurred until 1900. ^{137}Cs activity was
264 detected from 45.5 cm depth (4.2 ± 0.2 Bq.kg^{-1}) in the Malaguet sequence (Fig. 5). Maximal
265 concentration in this radionuclide was recorded at 15.5 cm depth (100.3 ± 2.4 Bq.kg^{-1}).
266 Log $^{210}Pb_{ex}$ activities significantly decreased with depth (r^2=0.88) – (Fig. 5). The CRS model
267 was applied to date this sequence that deposited between 1947 and 2017. Age models based
268 on $^{210}Pb_{ex}$ and ^{137}Cs were compared. The single peak of ^{137}Cs found was estimated to
269 correspond to 1986±1.2 years. The onset of the radiocesium deposits found at 45.5cm depth
270 was dated to 1955±2 years. Within the sequence, $^{210}Pb_{ex}$ activities showed the occurrence of
271 two periods of decrease of this radionuclide activities, first between 38.5 and 45.5 cm depth
272 (between 1963 and 1955) and then between 18.5 and 25.5 cm depth (corresponding to the
273 1981–1973 period).
274

3.4 Estimation of Mass Accumulation Rate (MAR) and the terrigenous fraction of sediment

Evolution of MAR in the Prugnolas pond shows a constant decrease of sediment delivery throughout time (MK test; p <0.001). Sediment supply to the lake decreased from 0.4 $g.cm^{-2}.yr^{-1}$ to 0.04 $g.cm^{-2}.yr^{-1}$ between 1907 and 2017 (Fig. 6). The period of maximum sediment input was recorded between 1900 and 1913, with an average rate of 0.3 ± 0.08 $g.cm^{-2}.yr^{-1.}$ This period was followed between 1913 and 1919 by a sharp decline of those inputs (average MAR = 0.18 ± 0.03 $g.cm^{-2}.yr^{-1}$). After the WWI, sediment delivery first increased slowly before decreasing significantly during the 1920s. From the 1960s onwards, sediment input decreased significantly from 0.1 $g.cm^{-2}.yr^{-1}$ in 1960 to 0.05 $g.cm^{-2}.yr^{-1}$ in 1965 (Fig. 6). The terrigenous fraction of sediment estimated based on the XRF data showed a similar trend as that of the total flux of sediment (MK test; <0,001). Relationship between MAR and the K/Ca ratio (used as a proxy for estimating the terrigenous fraction of sediment) was significant (r^2=0.66). This correlation suggests an accumulation of material produced by erosional processes occurring in the catchment. The 1900-1940 period corresponds to the period of maximal export of terrigenous material recorded in this sequence. However, during this phase, the terrigenous inputs decreased between 1908 and 1916, as observed for the MAR. From 1950 onwards, the inputs increased slowly before decreasing significantly in the early 1960s until the early 1980s. Then, the terrigenous inputs remained constant over time at a much lower level (Fig. 6).

For the Malaguet lake, MAR exhibited two distinct trends of material inputs (Fig. 7). First, the lower levels of the core (between 1951 and 1963) recorded the highest sediment input levels of the entire sequence (average MAR=0.6 ± 0.4 $g.cm^{-2}.yr^{-1}$). Within this large period, four specific levels were identified based on the ultra-high resolution Ct-scan data:

300 respectively in 1951-1953, 1954-1955, 1955-1959 and, finally, in 1961 (maximal MAR
301 values of these levels: 1.7; 0.92; 1.1; 0.7 $g.cm^{-2}.yr^{-1}$).
302 Then, in the upper part of the sequence corresponding to the period from the late 1960s to
303 2017, constant values of MAR over time were found (average MAR for this period =0.15 ±
304 0.06 $g.cm^{-2}.yr^{-1}$). From the second half of the 1950s, MAR exhibited a statically negative
305 trend (MK test: *p*-value <0.001). Similar trends were observed for the evolution of the
306 terrigenous fraction estimated based on the K/Ca proxy, except for the 1951-1953 period
307 where a additional peak of this fraction was detected. K/Ca ratio was strongly correlated to
308 the MAR values (r^2=0.84). This positive relationship demonstrates that the sediment supply to
309 the lake was dominated by soil erosion in the catchment.
310
311 **4. Discussion**
312 Results obtained in both catchments indicate the occurrence of a statistically
313 significant decline of sediment delivery and terrigenous inputs to the lakes of this region
314 throughout the 20th century. This decrease was observed during a period of major rural
315 depopulation and land cover change representative of those observed in other remote and rural
316 regions of France and Europe (Lasanta et al., 2017).
317 Sediment accumulation in the ponds decreased by 75% (Malaguet) to 99% (Prugnolas) during
318 the study period. These results are consistent with observations made in other catchments of
319 Eastern and Southern Europe. In Spain, farmland abandonment and land reforestation were
320 shown to have induced a decline of 54% in sediment yields (Boix-Fayos et al., 2008). In
321 Poland, erosion rates have decreased by 76% after land abandonment associated with
322 depopulation (Latocha et al., 2016). The same trend was observed in Slovenia (decline of 69%
323 of the total sediment delivery) - (Keesstra et al., 2009). However, these studies were all based
324 on model outputs (and not on field-based observations).

In the current research, the change in sediment delivery was strongly correlated to the decrease of the arable land surfaces (r^2=0.97 and r^2=0.94, respectively for the Prugnolas and Malaguet catchments) - (Fig. 8). Similar trends were observed in model-based studies conducted across Europe (e.g. Corbelle-Rico et al., 2012; Van Rompaey et al., 2007).

Furthermore, in the current research, land abandonment was strongly correlated to the rate of depopulation (r^2=0.91 and 0.86 respectively for Prugnolas and Malaguet)– (Fig. 8). This corroborates previous results on the link between depopulation and land abandonment obtained in Eastern Europe or in the Mediterranean region (e.g. Kosmas et al., 2015; Pazúr et al., 2014).

The detailed chronology of population and land use change in the two catchments investigated in the current research showed that the strongest changes occurred during the post-WWII period. After 1945, a significant movement of land abandonment by farmers was observed in this rural region. Before leaving, farmers planted trees in their arable land to provide them an additional source of income. In addition of these local reforestation operations, the French authorities have financially supported afforestation programmes in many areas of the Massif-Central region. These operations mainly took place between 1945 and 1970. The physiognomy of Massif-Central landscapes drastically changed, from a dominance of bare ground areas to one of the densest forested areas in France. In addition to these afforestation works, spontaneous reforestation occurred in abandoned cropland. At the French scale, 4.5 million hectares were reforested (corresponding to 30% of the surface of French forests by 2000, i.e. 8% of the French territory) as a result of coordinated operations and natural regrowth after land abandonment between 1945 and 1999. The Massif-Central region is one of the most reforested areas in France (Dodane, 2009).

Surprisingly, in the Malaguet catchment, afforestation periods correspond to the main sediment input phases into the lake. Afforestation works were already described as a potential

350 factor accelerating soil erosion rates (e.g. Romero-Diaz et al., 2010). Detritical pulses
351 detected in the Malaguet sediment core were associated with a decrease in the sediment
352 $^{210}Pb_{ex}$ activities. This may reflect the preferential mobilization of subsoil material sheltered
353 from atmospheric fallout and depleted in fallout radionuclides (Evrard et al., 2016a; Foucher
354 et al., 2015; Laceby et al., 2017; Le Gall et al., 2017) during these operations and further
355 supports the hypothesis of major landscape disturbances, which would have occurred between
356 1950 and 1970 in this catchment (e.g. Simms et al., 2008). After this extensive land use
357 conversion, soil erosion rates decreased from a mean of 135 $t.km^{-2}.year^{-1}$ between 1945-1950
358 to a mean of 28 $t.km^{-2}.year^{-1}$ between 2000-2017. Maximal erosion rates were recorded at the
359 onset of the different phases of afforestation within these catchments, with the occurrence of
360 four detrital layers (250, 240, 280 and 210 $t.km^{-2}.year^{-1}$, estimated to have deposited in 1951-
361 1953, 1954-1955, 1956-1959 and 1961, respectively). These layers were likely associated
362 with the occurrence of major land use changes, or afforestation works in the area draining to
363 the lake.
364 Approximately 15 years after the completion of the afforestation programmes, sediment
365 export tended to stabilize with the widespread development of forest canopy and the hillslope
366 stabilization (with the root growth and the increase in the soil cover by vegetation). Similar
367 observations were made in an afforested site of Scotland (Battarbee et al., 1985). Sediment
368 accumulation increased ten-fold during this disturbance period, and it then returned to the pre-
369 afforestation levels after about 10 years.
370 In the Prugnolas catchment, afforestation works were less extensive and they mainly
371 took place in upper catchment parts, in areas that are not well connected to the lake.
372 Furthermore, this process mainly resulted from the natural regrowth of trees on abandoned
373 agricultural land. Accordingly, in this context, the impact of reforestation on soil erosion rates
374 remained low, with the exception of a slight increase of the terrigenous inputs into the lake

375 between 1945 and 1980. However, despite this limited increase, the sediment accumulation
376 sequence recorded in this core illustrates the sedimentation in a lake draining a relatively
377 undisturbed natural catchment compared to the situation observed in the Malaguet lake, where
378 larger changes in sediment inputs were observed in response to both natural and
379 anthropogenic changes in the drainage area.
380 We would like to thank the reviewer for this valuable suggestion. Comparison with studies
381 compiling erosion rates in similar environments were added to the discussion section
382 (LL.375-389).
383 In contrast to the two sites impacted by land abandonment investigated in the current
384 research, other basins with similar initial land uses were affected by distinct soil erosion
385 trajectories. In the UK, Foster and Lee (1999) summarized a large number of these trajectories
386 deduced from the analysis of sedimentary sequences. For instance, sediment cores collected in
387 the Silsden reservoir (Yorkshire) underwent a three-fold higher sediment supply in 1990
388 compared to that observed at the end of the 19th century. As no major change in the arable
389 land proportion was observed in the drainage area, this accelerated sediment supply was
390 attributed to the increased surface areas covered with grassland for both sheep and cattle
391 grazing. A similar trend was recorded in the Elleron lake (Yorkshire) where sheep and cattle
392 grazing have led to a two-fold increase of the sediment production during the 20th century,
393 without any significant change in the arable land surface area. In contrast, in catchments
394 impacted by land use change (transition from grassland to arable land) as in that of Fillingham
395 lake (East Midlands), sediment production increased 5-fold after agricultural intensification.
396 Similar dynamics were recorded in the Yetlhom lake (East Midlands) where grassland was
397 massively converted into arable land (after 1921). These changes increased sediment delivery
398 from 22 times.

399 In contrast to the well-documented great acceleration of soil erosion observed during
400 the 20th century in agricultural plains (Foucher et al., 2014; N. Ramankutty and Foley, 1999),
401 relatively few studies quantified this opposite trajectory of soil erosion decrease in response to
402 land abandonment. The surface of abandoned land should increase across the world during the
403 21th century. Existing data estimated the extent of farmland abandonment in 2030 to 3-4% of
404 the currently utilized agricultural area in Europe (corresponding to 126,000-168,000 km²) -
405 (Keenleyside and Tucker, 2010). In Japan, official statistics estimated the total abandonment
406 rate of cropland at 10.6% in 2010 (Osawa et al., 2015). In eastern Europe between 15 and
407 20% of cropland areas have been abandoned since the 1980's. In post-soviet Russia, more
408 than 40 million hectares of arable lands were abandoned (Rosstat, 2010). In Western Europe,
409 rate of land abandonment is estimated to 0.17% in France and 0.8% in Spain (Pointereau et
410 al., 2008).
411 Return to cultivation of this abandoned land is very difficult or even not feasible for
412 economic reasons (Corbelle-Rico and Crecente-Maseda, 2008). The two land use conversion
413 patterns (deforestation for intensive agriculture and land abandonment) will likely not balance
414 each other in the next future decades. Accordingly, a better quantification of the processes
415 that occurred in these areas remains a challenge to improve estimations of the global soil
416 erosion budget and its spatial and temporal variations.
417
418 **Conclusions**
419
420 The investigation of sediment accumulation in lakes provides a powerful technique for
421 reconstructing the impact of human activities on soil erosion rates. Although lake deposits
422 were extensively used in high altitude regions (e.g. in the Alps) for quantifying the impact of
423 the agricultural expansion and its subsequent abandonment on soil erosion, very few records

424 are available to investigate the impact of these changes in remote and rural highland areas.
425 The current research quantified the occurrence of a significant decline of sediment delivery
426 and terrigenous inputs to the lakes of remote and rural highland areas of western Europe,
427 throughout the 20th century. In 100 years, sediment production has decreased of 75 to 99% in
428 these areas. This general decrease was observed during a period of major rural depopulation
429 and the associated land cover change, with a massive conversion of arable land into forests.
430 These results showed how complex soil erosion trajectories may be at the regional scale.
431 These processes that are often neglected in the current soil erosion investigations should be
432 better taken into account for improving modelling approaches and designing sustainable
433 strategies of land use management and food security in a world in demographic expansion.
434

435 **Acknowledgements**

436 The authors are grateful to Anne Colmar, Xavier Bourrain and Jean-Noël Gautier for
437 their technical and financial support. This work was supported by a grant from the Loire-
438 Brittany Water Agency (METEOR project). The authors would also like to thank Jerome
439 Vany (Office National des Forêts), Peggy Chevilley (Communauté de Commune de
440 Bourganeuf) and Nathanaël Lefèvre (PNR Livradois-Forez) for their precious help to obtain
441 historical data on the studied catchments. Authors also gratefully acknowledge Naresh Kumar
442 and Anastasiia Bagaeva for their help during field surveys.
443

444 References

445 Antrop, M., 2005. Why landscapes of the past are important for the future. Landsc. Urban
446 Plan. 70, 21–34. https://doi.org/http://dx.doi.org/10.1016/j.landurbplan.2003.10.002

447 Appleby, P.G., Oldfield, F., 1978. The calculation of lead-210 dates assuming a constant rate

448 of supply of unsupported210Pb to the sediment. Catena 5, 1–8.
449 https://doi.org/10.1016/S0341-8162(78)80002-2

450 Arnaez, J., Lasanta, T., Errea, M.P., Ortigosa, L., 2011. Land abandonment, landscape
451 evolution, and soil erosion in a Spanish Mediterranean mountain region: The case of
452 Camero Viejo. L. Degrad. Dev. 22, 537–550. https://doi.org/10.1002/ldr.1032

453 Bajard, M., Sabatier, P., David, F., Develle, A.L., Reyss, J.L., Fanget, B., Malet, E., Arnaud,
454 D., Augustin, L., Crouzet, C., Poulenard, J., Arnaud, F., 2016. Erosion record in Lake La
455 Thuile sediments (Prealps, France): Evidence of montane landscape dynamics
456 throughout the Holocene. Holocene. https://doi.org/10.1177/0959683615609750

457 Battarbee, R.W., Appleby, P.G., Odell, K., Flower, R.J., 1985. 210Pb dating of scottish lake
458 sediments, afforestation and accelerated soil erosion. Earth Surf. Process. Landforms.
459 https://doi.org/10.1002/esp.3290100206

460 Boardman, J., Poesen, J., 2006. Soil Erosion in Europe, Soil Erosion in Europe.
461 https://doi.org/10.1002/0470859202

462 Boix-Fayos, C., de Vente, J., Martínez-Mena, M., Barberá, G.G., Castillo, V., 2008. The
463 impact of land use change and check-dams on catchment sediment yield. Hydrol.
464 Process. https://doi.org/10.1002/hyp.7115

465 Buishand, T.A., 1982. Some methods for testing the homogeneity of rainfall records. J.
466 Hydrol. https://doi.org/10.1016/0022-1694(82)90066-X

467 Campbell, J.E., Lobell, D.B., Genova, R.C., Field, C.B., 2008. The global potential of
468 bioenergy on abandoned agriculture lands. Environ. Sci. Technol.
469 https://doi.org/10.1021/es800052w

470 Corbelle-Rico, E., Crecente-Maseda, R., 2008. Abandonment of agricultural land: an

471 overview of drivers and consequences. Rev. Galega Econ. 17.

472 Corbelle-Rico, E., Crecente-Maseda, R., Santé-Riveira, I., 2012. Multi-scale assessment and
473 spatial modelling of agricultural land abandonment in a European peripheral region:
474 Galicia (Spain), 1956–2004. Land use policy 29, 493–501.
475 https://doi.org/10.1016/j.landusepol.2011.08.008

476 Cramer, V.A., Hobbs, R.J., Society for Ecological Restoration International., 2007. Old
477 fields : dynamics and restoration of abandoned farmland, The science and practice of
478 ecological restoration.

479 Cramer, V.A., Hobbs, R.J., Standish, R.J., 2008. What's new about old fields? Land
480 abandonment and ecosystem assembly. Trends Ecol. Evol.
481 https://doi.org/10.1016/j.tree.2007.10.005

482 Croudace, I.W., Rothwell, R.G., 2015. Micro-XRF Studies of Sediment Cores: Applications
483 of a non-destructive tool for the environmental sciences, Developments in
484 Paleoenvironmental Research. https://doi.org/10.1007/978-94-017-9849-5

485 Dearing, J.A., Jones, R.T., 2003. Coupling temporal and spatial dimensions of global
486 sediment flux through lake and marine sediment records. Glob. Planet. Change 39, 147–
487 168. https://doi.org/http://dx.doi.org/10.1016/S0921-8181(03)00022-5

488 Dodane, C., 2009. Les nouvelles forêts du Massif Central: enjeux sociétaux et territoriaux.
489 Ces hommes qui plantaient des résineux pour éviter la friche.

490 Evrard, O., Laceby, J.P., Huon, S., Lefèvre, I., Sengtaheuanghoung, O., Ribolzi, O., 2016a.
491 Combining multiple fallout radionuclides (137Cs,7Be,210Pbxs) to investigate temporal
492 sediment source dynamics in tropical, ephemeral riverine systems. J. Soils Sediments.
493 https://doi.org/10.1007/s11368-015-1316-y

494 Evrard, O., Laceby, J.P., Onda, Y., Wakiyama, Y., Jaegler, H., Lefèvre, I., 2016b.
495 Quantifying the dilution of the radiocesium contamination in Fukushima coastal river
496 sediment (2011–2015). Sci. Rep. 6, 34828. https://doi.org/10.1038/srep34828

497 Feder, G., Umali, D.L., 1993. The adoption of agricultural innovations. A review. Technol.
498 Forecast. Soc. Change. https://doi.org/10.1016/0040-1625(93)90053-A

499 Foley, J.A., Defries, R., Asner, G., Barford, C., Bonan, G., Carpenter, S., Chapin, F., Coe, M.,
500 Daily, G., Gibbs, H., Helkowski, J., Holloway, T., Howard, E., Kucharik, C., Monfreda,
501 C., Patz, J., Prentice, I., Ramankutty, N., Snyder, P., 2005. Global Consequences of Land
502 Use. Science (80-.). 309, 570–574. https://doi.org/10.1126/science.1111772

503 Foucher, A., Le Gall, M., Salvador blanes, S., Evrard, O., Cerdan, O., Laceby, J.P.,
504 Vandromme, R., Lefevre, I., Maniere, L., Grangeon, T., Bakyono, J.P., Desmet, M.,
505 2017. Increase of erosion source contributions to rivers and lakes (1950 2010): The case
506 of the Louroux Pond (Central France). Houille Blanche 2017–Decem.
507 https://doi.org/10.1051/lhb/2017051

508 Foucher, A., Patrick Laceby, J., Salvador-Blanes, S., Evrard, O., Le Gall, M., Lefèvre, I.,
509 Cerdan, O., Rajkumar, V., Desmet, M., 2015. Quantifying the dominant sources of
510 sediment in a drained lowland agricultural catchment: The application of a thorium-
511 based particle size correction in sediment fingerprinting. Geomorphology.
512 https://doi.org/10.1016/j.geomorph.2015.09.007

513 Foucher, A., Salvador-Blanes, S., Evrard, O., Simonneau, A., Chapron, E., Courp, T., Cerdan,
514 O., Lefèvre, I., Adriaensen, H., Lecompte, F., Desmet, M., 2014. Increase in soil erosion
515 after agricultural intensification: Evidence from a lowland basin in France. Anthropocene
516 7, 30–41. https://doi.org/10.1016/j.ancene.2015.02.001

517 García-Ruiz, J.M., Lana-Renault, N., 2011. Hydrological and erosive consequences of

518 farmland abandonment in Europe, with special reference to the Mediterranean region - A
519 review. Agric. Ecosyst. Environ. https://doi.org/10.1016/j.agee.2011.01.003

520 Giguet-Covex, C., Arnaud, F., Poulenard, J., Disnar, J.-R., Delhon, C., Francus, P., David, F.,
521 Enters, D., Rey, P.-J., Delannoy, J.-J., 2011. Changes in erosion patterns during the
522 Holocene in a currently treeless subalpine catchment inferred from lake sediment
523 geochemistry (Lake Anterne, 2063 m a.s.l., NW French Alps): The role of climate and
524 human activities. The Holocene 21, 651–665.
525 https://doi.org/10.1177/0959683610391320

526 Heathcote, A.J., Filstrup, C.T., Downing, J.A., 2013. Watershed Sediment Losses to Lakes
527 Accelerating Despite Agricultural Soil Conservation Efforts. PLoS One 8, e53554.
528 https://doi.org/10.1371/journal.pone.0053554

529 Hill, J., Stellmes, M., Udelhoven, T., Röder, A., Sommer, S., 2008. Mediterranean
530 desertification and land degradation. Mapping related land use change syndromes based
531 on satellite observations. Glob. Planet. Change.
532 https://doi.org/10.1016/j.gloplacha.2008.10.005

533 INRA, 2015. Référentiel régional pédologique du Limousin à 1/250 000e. Régions naturelles,
534 pédopaysages et sols.

535 IUSS Working Group WRB, 2015. World Reference Base for Soil Resources 2014, update
536 2015. International soil classification system for naming soils and creating legends for
537 soil maps., World Soil Resources Reports No. 106.

538 Keenleyside, C., Tucker, G., 2010. Farmland abandonment in the EU: an assessment of trends
539 and prospects. Rep. Prep. WWF, Inst. Eur. Environ. Policy.
540 https://doi.org/10.1016/j.outlook.2010.06.002

Keesstra, S.D., van Dam, O., Verstraeten, G., van Huissteden, J., 2009. Changing sediment dynamics due to natural reforestation in the Dragonja catchment, SW Slovenia. Catena. https://doi.org/10.1016/j.catena.2009.02.021

Klein Goldewijk, K., Beusen, A., Doelman, J., Stehfest, E., 2016. New anthropogenic land use estimates for the Holocene; HYDE 3.2. Earth Syst. Sci. Data Discuss. 1–40. https://doi.org/10.5194/essd-2016-58

Kosmas, C., Danalatos, N., Cammeraat, L.H., Chabart, M., Diamantopoulos, J., Farand, R., Gutierrez, L., Jacob, A., Marques, H., Martinez-Fernandez, J., Mizara, A., Moustakas, N., Nicolau, J.M., Oliveros, C., Pinna, G., Puddu, R., Puigdefabregas, J., Roxo, M., Simao, A., Stamou, G., Tomasi, N., Usai, D., Vacca, A., 1997. The effect of land use on runoff and soil erosion rates under Mediterranean conditions. Catena. https://doi.org/10.1016/S0341-8162(96)00062-8

Kosmas, C., Kairis, O., Karavitis, C., Acikalin, S., Alcalá, M., Alfama, P., Atlhopheng, J., Barrera, J., Belgacem, A., Solé-Benet, A., Brito, J., Chaker, M., Chanda, R., Darkoh, M., Ermolaeva, O., Fassouli, V., Fernandez, F., Gokceoglu, C., Gonzalez, D., Gungor, H., Hessel, R., Khatteli, H., Khitrov, N., Kounalaki, A., Laouina, A., Magole, L., Medina, L., Mendoza, M., Mulale, K., Ocakoglu, F., Ouessar, M., Ovalle, C., Perez, C., Perkins, J., Pozo, A., Prat, C., Ramos, A., Ramos, J., Riquelme, J., Ritsema, C., Romanenkov, V., Sebego, R., Sghaier, M., Silva, N., Sizemskaya, M., Sonmez, H., Taamallah, H., Tezcan, L., de Vente, J., Zagal, E., Zeiliguer, A., Salvati, L., 2015. An exploratory analysis of land abandonment drivers in areas prone to desertification. CATENA 128, 252–261. https://doi.org/10.1016/j.catena.2014.02.006

Koulouri, M., Giourga, C., 2007. Land abandonment and slope gradient as key factors of soil erosion in Mediterranean terraced lands. Catena.

https://doi.org/10.1016/j.catena.2006.07.001

Laceby, J.P., Evrard, O., Smith, H.G., Blake, W.H., Olley, J.M., Minella, J.P.G., Owens, P.N., 2017. The challenges and opportunities of addressing particle size effects in sediment source fingerprinting: A review. Earth-Science Rev. https://doi.org/10.1016/j.earscirev.2017.04.009

Lasanta, T., Arnáez, J., Pascual, N., Ruiz-Flaño, P., Errea, M.P., Lana-Renault, N., 2017. Space–time process and drivers of land abandonment in Europe. Catena. https://doi.org/10.1016/j.catena.2016.02.024

Latocha, A., Szymanowski, M., Jeziorska, J., Stec, M., Roszczewska, M., 2016. Effects of land abandonment and climate change on soil erosion-An example from depopulated agricultural lands in the Sudetes Mts., SW Poland. Catena. https://doi.org/10.1016/j.catena.2016.05.027

Le Gall, M., Evrard, O., Foucher, A., Laceby, J.P., Salvador-Blanes, S., Manière, L., Lefèvre, I., Cerdan, O., Ayrault, S., 2017. Investigating the temporal dynamics of suspended sediment during flood events with 7 Be and 210 Pb xs measurements in a drained lowland catchment. Sci. Rep. 7. https://doi.org/10.1038/srep42099

Lesiv, M., Schepaschenko, D., Moltchanova, E., Bun, R., Dürauer, M., Prishchepov, A. V., Schierhorn, F., Estel, S., Kuemmerle, T., Alcántara, C., Kussul, N., Shchepashchenko, M., Kutovaya, O., Martynenko, O., Karminov, V., Shvidenko, A., Havlik, P., Kraxner, F., See, L., Fritz, S., 2018. Data descriptor: Spatial distribution of arable and abandoned land across former Soviet Union countries. Sci. Data. https://doi.org/10.1038/sdata.2018.56

Lesschen, J.P., Cammeraat, L.H., Nieman, T., 2008. Erosion and terrace failure due to agricultural land abandonment in a semi-arid environment. Earth Surf. Process.

589 Landforms. https://doi.org/10.1002/esp.1676

590 Novara, A., Gristina, L., Sala, G., Galati, A., Crescimanno, M., Cerdà, A., Badalamenti, E.,
591 La Mantia, T., 2017. Agricultural land abandonment in Mediterranean environment
592 provides ecosystem services via soil carbon sequestration. Sci. Total Environ.
593 https://doi.org/10.1016/j.scitotenv.2016.10.123

594 Osawa, T., Kadoya, T., Kohyama, K., 2015. 5- and 10-km mesh datasets of agricultural land
595 use based on governmental statistics for 1970–2005. Ecol. Res.
596 https://doi.org/10.1007/s11284-015-1290-2

597 Pazúr, R., Lieskovský, J., Feranec, J., Oťaheľ, J., 2014. Spatial determinants of abandonment
598 of large-scale arable lands and managed grasslands in Slovakia during the periods of
599 post-socialist transition and European Union accession. Appl. Geogr. 54, 118–128.
600 https://doi.org/10.1016/j.apgeog.2014.07.014

601 Plieninger, T., Hui, C., Gaertner, M., Huntsinger, L., 2014. The impact of land abandonment
602 on species richness and abundance in the Mediterranean Basin: A meta-analysis. PLoS
603 One. https://doi.org/10.1371/journal.pone.0098355

604 Pointereau, P., Coulon, F., Girard, P., Lambotte, M., Stuczynski, T., Sánchez Ortega, V., Del
605 Rio, A., 2008. Analysis of the Driving Forces behind Farmland Abandonment and the
606 Extent and Location of Agricultural Areas that are Actually Abandoned or are in Risk to
607 be Abandoned, JCR Scientific and Technical reports.
608 https://doi.org/10.13140/RG.2.1.2467.7849

609 Queiroz, C., Beilin, R., Folke, C., Lindborg, R., 2014. Farmland abandonment: Threat or
610 opportunity for biodiversity conservation? A global review. Front. Ecol. Environ.
611 https://doi.org/10.1890/120348

612 Ramankutty, N., Foley, J.A., 1999. Estimating historical changes in land cover North
613 American croplands from 1850 to 1992. Glob. Ecol. Biogeogr.
614 https://doi.org/10.1046/j.1365-2699.1999.00141.x

615 Ramankutty, N., Foley, J.A., 1999. Estimating historical changes in global land cover:
616 Croplands from 1700 to 1992. Global Biogeochem. Cycles.
617 https://doi.org/10.1029/1999GB900046

618 Rodrigo-Comino, J., Martinez-Hernandez, C., Iserloh, T., Cerda, A., 2018. Contrasted Impact
619 of Land Abandonment on Soil Erosion in Mediterranean Agriculture Fields. Pedosphere.
620 https://doi.org/10.1016/S1002-0160(17)60441-7

621 Romero-Diaz, A., Belmonte-Serrato, F., Ruiz-Sinoga, J.D., 2010. The geomorphic impact of
622 afforestations on soil erosion in southeast spain. L. Degrad. Dev.
623 https://doi.org/10.1002/ldr.946

624 Rosstat, 2010. Regions of Russia. Socio-Economic Measures (Regiony Rossii. Sotsio-
625 ekonomicheskie Pokazateli) (Moscow: Russian Federal Service of State Statistics).

626 Schierhorn, F., Müller, D., Beringer, T., Prishchepov, A. V., Kuemmerle, T., Balmann, A.,
627 2013. Post-Soviet cropland abandonment and carbon sequestration in European Russia,
628 Ukraine, and Belarus. Global Biogeochem. Cycles.
629 https://doi.org/10.1002/2013GB004654

630 Schneider, C.A., Rasband, W.S., Eliceiri, K.W., 2012. NIH Image to ImageJ: 25 years of
631 image analysis. Nat. Methods 9, 671–675. https://doi.org/10.1038/nmeth.2089

632 Simms, A.D., Woodroffe, C., Jones, B.G., Heijnis, H., Mann, R.A., Harrison, J., 2008. Use of
633 210Pb and 137Cs to simultaneously constrain ages and sources of post-dam sediments in
634 the Cordeaux reservoir, Sydney, Australia. J. Environ. Radioact. 99, 1111–1120.

https://doi.org/10.1016/j.jenvrad.2008.01.002

Van Rompaey, A., Krasa, J., Dostal, T., 2007. Modelling the impact of land cover changes in the Czech Republic on sediment delivery. Land use policy 24, 576–583. https://doi.org/10.1016/j.landusepol.2005.10.003

Warren, J., Gilbert, R.O., 1988. Statistical Methods for Environmental Pollution Monitoring. Technometrics. https://doi.org/10.2307/1270090

Figures

Fig. 1: (a) Localization map of the study sites within the Loire River basin (PG= Prugnolas site, MA = Malaguet site), (b) detailed map of the Prugnolas catchment, (c) detailed map of the Malaguet catchment, (d), Prugnolas pond characteristics and core sampling location, (e) Malaguet lake characteristics and core sampling location.

Fig. 2: Evolution of the population in the Prugnolas and Malaguet catchments during the 20^{th} century

Fig. 3: Evolution of the main land uses between 1948 and 2010 in the Prugnolas and Malaguet catchments based on the analysis of aerial images and agricultural census data. Grey areas correspond to the afforestation periods.

Fig. 4: Illustration of the spatial pattern of land use change in the Prugnolas catchment between 1950 and 2000. Land use was estimated from on digitized aerial images.

Fig. 5: Age model of the 43-MA-1703 core (Malaguet lake) based on the fallout radionuclide activity measurements.

Fig. 6: Evolution of the mass accumulation rate and the terrigenous material input fraction estimated from the changes in K/Ca ratio based on XRF measurements in the sediment core collected in the Prugnolas pond.

Fig. 7: Evolution of the mass accumulation rate and the terrigenous material input fraction estimated from the changes in K/Ca ratio based on XRF measurements in the sediment core collected in the Malaguet lake.

Fig. 8: Comparison between average Mass Accumulation Rate, evolution of population and proportion of arable land for the Malaguet and Prugnolas catchment

Supplementary material:

Table 1: Evolution of land use in the Prugnolas catchment between 1950 and 2010. *correspond to land use estimated by the analysis of aerial images

684 Table 2: Evolution of land use in the Malaguet catchment between 1950 and 2010

685 *correspond to land use estimated by the analysis aerial imageries

686

Table 1

Click here to download Tables: table1.docx

	2010	2000	*2000**	1988	1979	*1979**	*1972**	1970	1955	*1950**
Arable land (%)	16	13	*12*	18	20	*26*		20	47	*68*
Cropland (%)	0,4	0,7	*0,9*	1,7	2,4	*3,6*		3,3	5,5	*7,3*
Grassland (%)	16	13	*11*	16	17	*23*		17	42	*61*
Permanent (%	14	10	-	15	16	-		13	-	-
temporary (%)	2	2	-	1	2	-		3	-	-
Forest (%)	82	85	*86*	80	78	*72*		78	51	*30*
Other	2	2	*2*	2	2	*2*		2	2	*2*
Urban area (%)	2	2	*2*	2	1	*1*		1	1	*1*
Water body (%)	0,5	0,5	*0,5*	0,5	0,5	*0,5*		0,5	0,5	*0,5*

Table 2

Click here to download Tables: table 2.docx

	2010	**2000**	***1995****	**1988**	**1979**	***1977****	***1970***	***1967****	***1955****	***1948****
Arable land (%)	15	18	*21*	23	28	*33*	38	*39*	*44*	*45*
Cropland (%)	2	3	*5*	5	7	*8*	9	*13*	*14*	*13*
Grassland (%)	13	14	*17*	18	19	*25*	28	*26*	*29*	*33*
Forest (%)	71	69	*65*	64	62	*55*	51	*50*	*45*	*43*
Other	13	13	*13*	13	12	*12*	*12*	*12*	*12*	*12*
Urban area (%)	6	6	*6*	6	6	*6*	5	*5*	*5*	*5*
Water body (%)	7	7	*7*	7	7	*7*	6	*6*	*6*	*6*

Fig. 1

Click here to download high resolution image

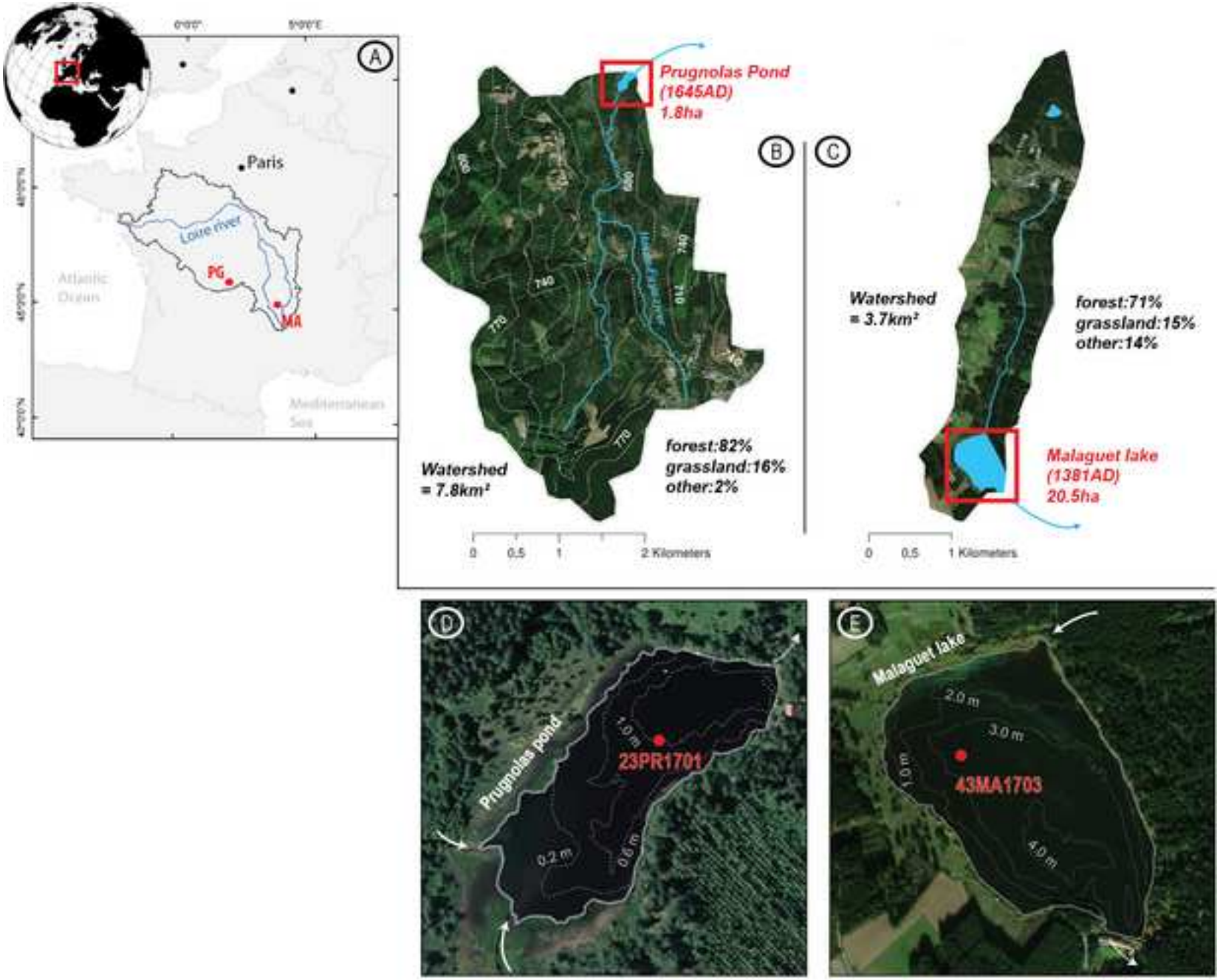

Fig. 2

Click here to download high resolution image

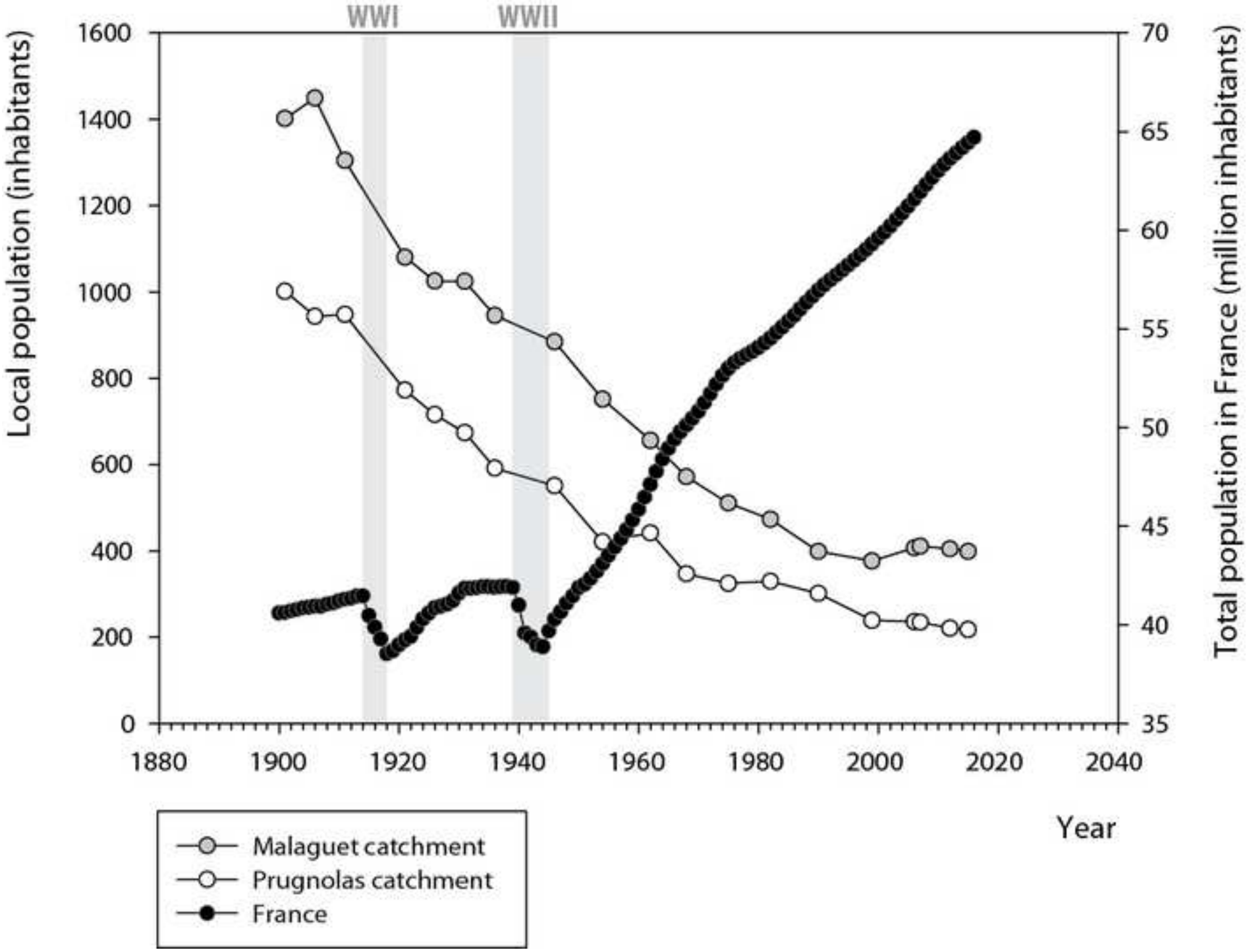

Fig. 3

Click here to download high resolution image

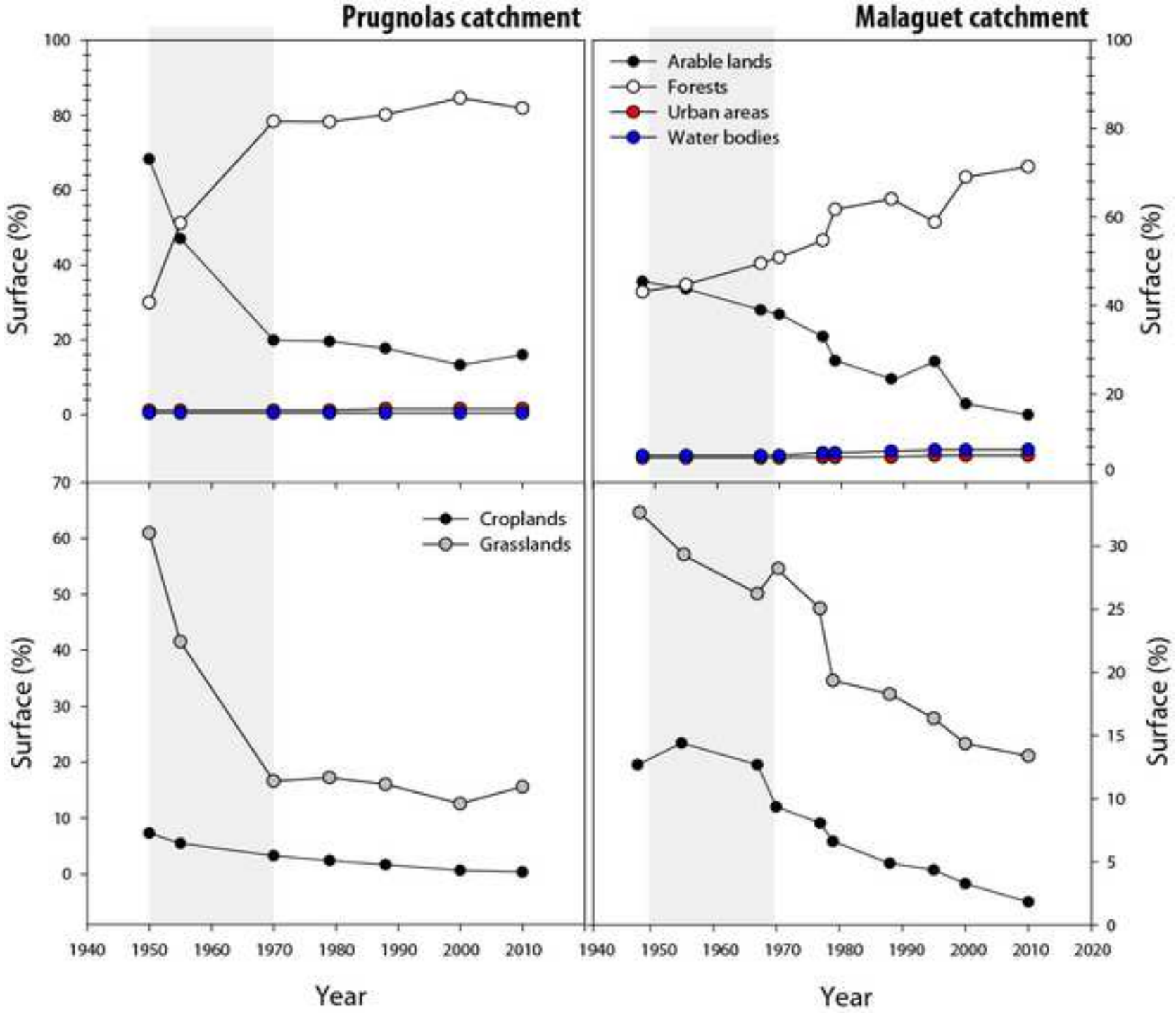

Fig. 4

Click here to download high resolution image

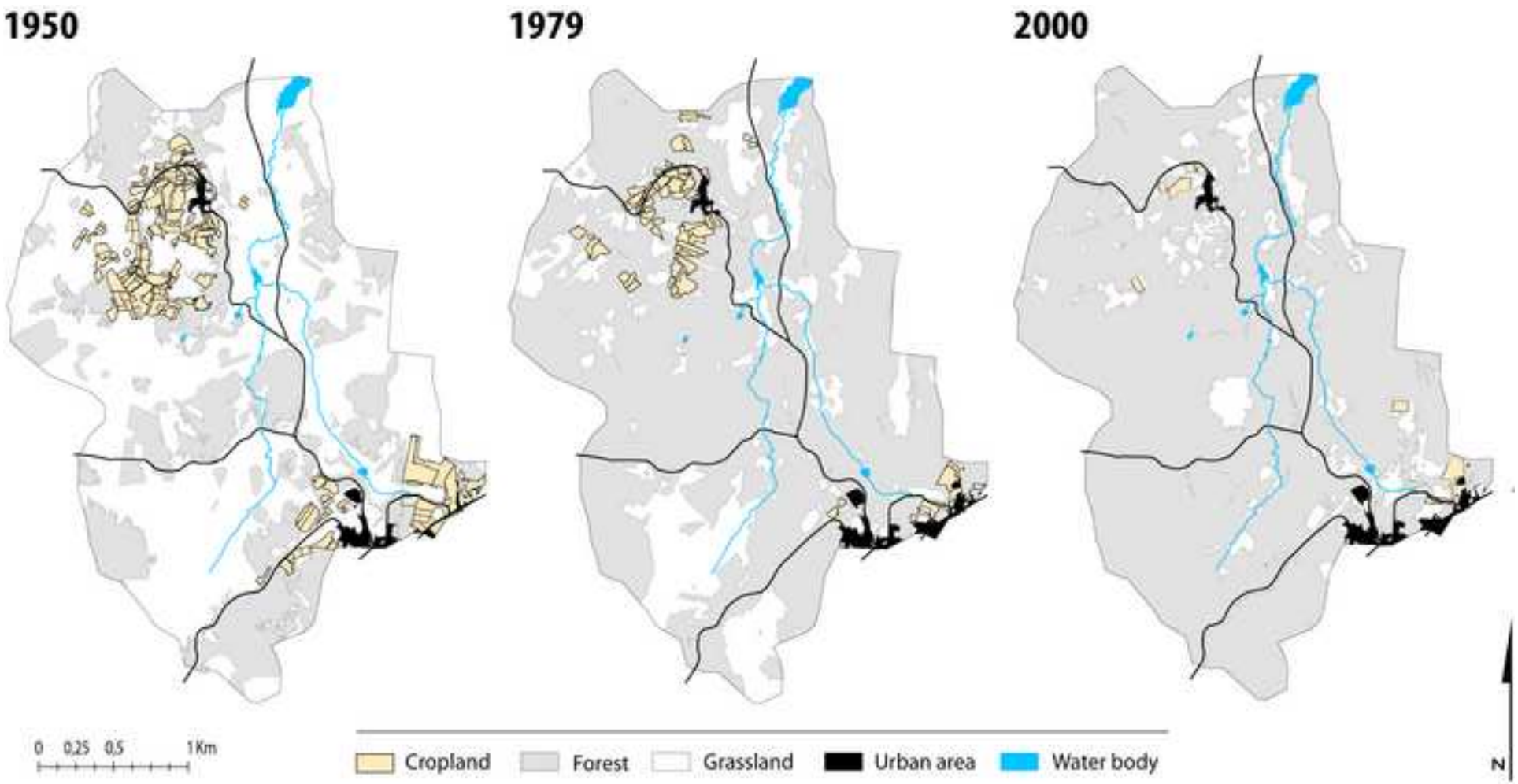

Fig. 5

Click here to download high resolution image

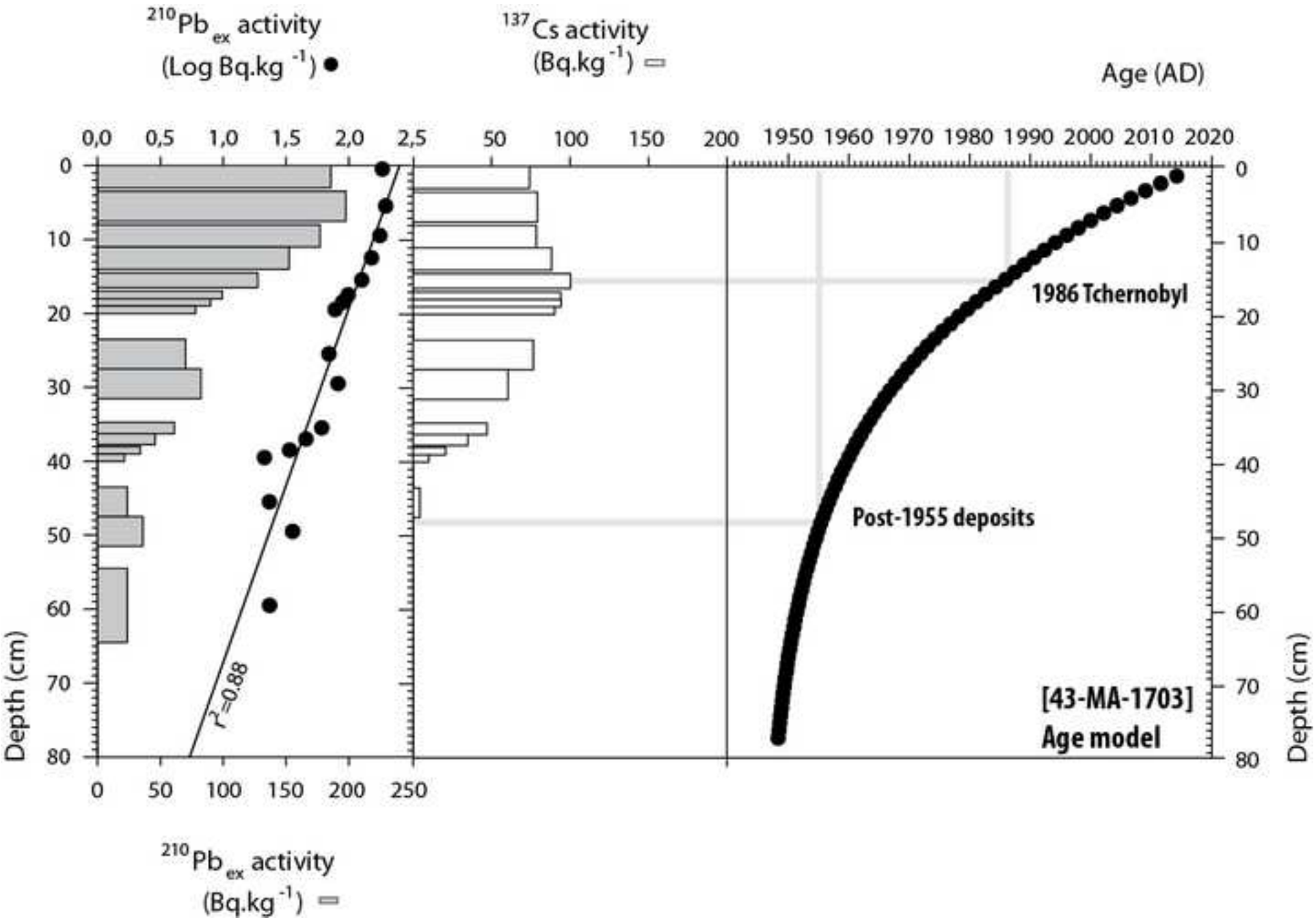

Fig. 6

Click here to download high resolution image

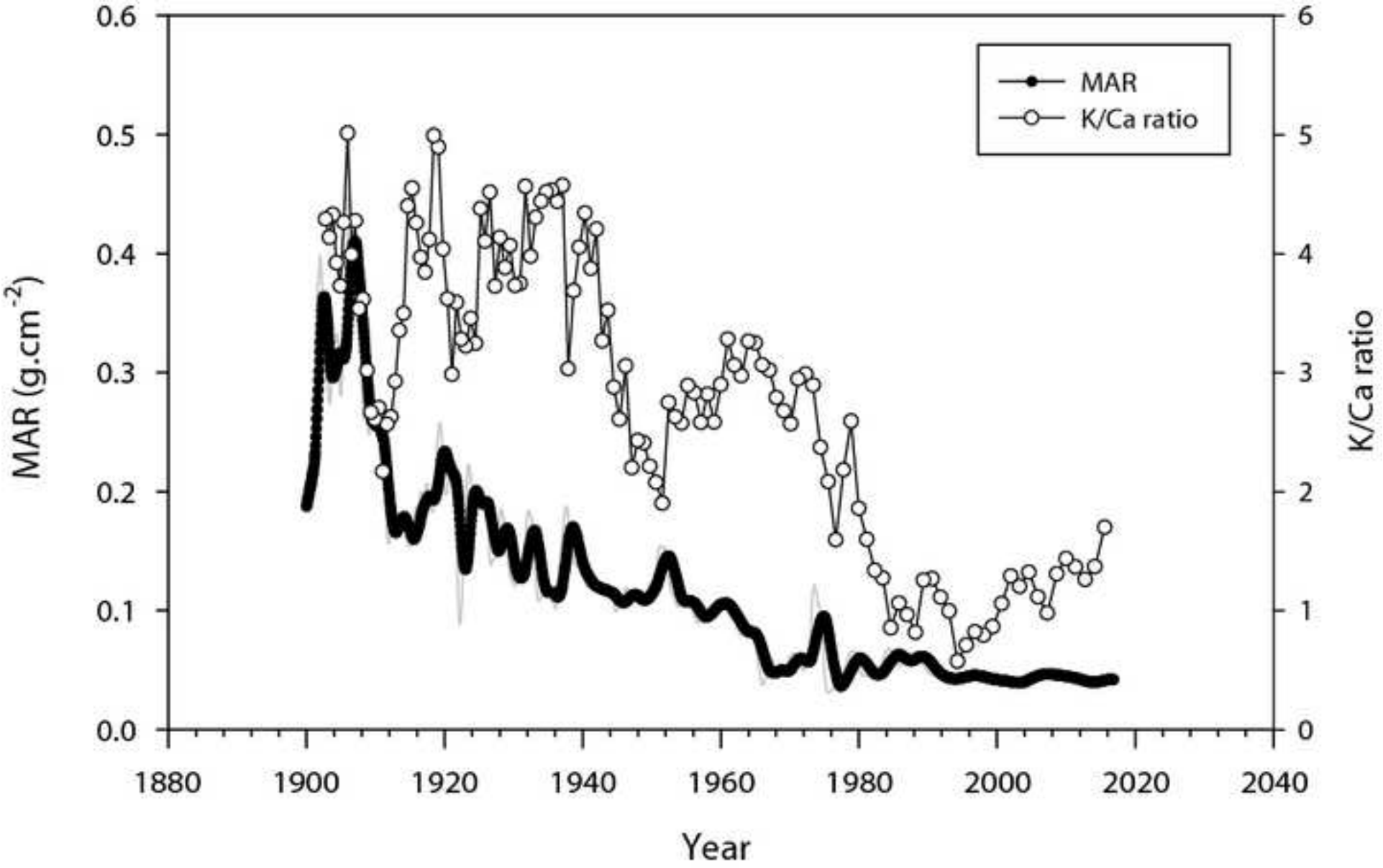

Fig. 7

Click here to download high resolution image

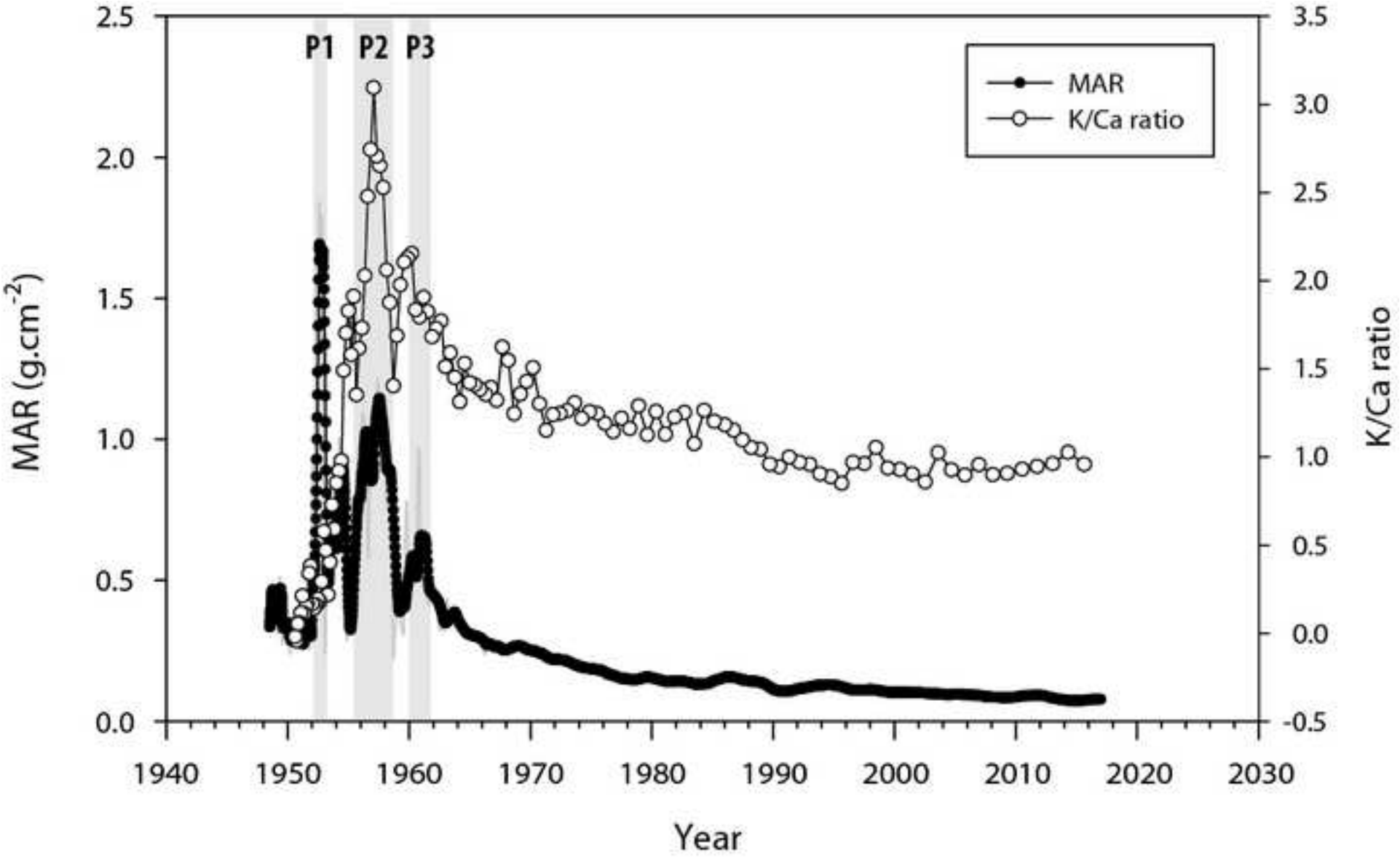

Fig. 8

Click here to download high resolution image